The vibrational dependence of dissociative recombination: Rate constants for N 2 +

Steven L. Guberman

Citation: The Journal of Chemical Physics **141**, 204307 (2014); doi: 10.1063/1.4901892
View online: http://dx.doi.org/10.1063/1.4901892
View Table of Contents: http://scitation.aip.org/content/aip/journal/jcp/141/20?ver=pdfcov
Published by the AIP Publishing

The vibrational dependence of dissociative recombination: Rate constants for N_2^+

Steven L. Guberman[a)]
Institute for Scientific Research, 22 Bonad Road, Winchester, Massachusetts 01890, USA

(Received 26 August 2014; accepted 3 November 2014; published online 25 November 2014)

Dissociative recombination rate constants are reported with electron temperature dependent uncertainties for the lowest 5 vibrational levels of the N_2^+ ground state. The rate constants are determined from *ab initio* calculations of potential curves, electronic widths, quantum defects, and cross sections. At 100 K electron temperature, the rate constants overlap with the exception of the third vibrational level. At and above 300 K, the rate constants for excited vibrational levels are significantly smaller than that for the ground level. It is shown that any experimentally determined total rate constant at 300 K electron temperature that is smaller than 2.0×10^{-7} cm^3/s is likely to be for ions that have a substantially excited vibrational population. Using the vibrational level specific rate constants, the total rate constant is in very good agreement with that for an excited vibrational distribution found in a storage ring experiment. It is also shown that a prior analysis of a laser induced fluorescence experiment is quantitatively flawed due to the need to account for reactions with unknown rate constants. Two prior calculations of the dissociative recombination rate constant are shown to be inconsistent with the cross sections upon which they are based. The rate constants calculated here contribute to the resolution of a 30 year old disagreement between modeled and observed N_2^+ ionospheric densities.
 [http://dx.doi.org/10.1063/1.4901892]

I. INTRODUCTION

Starting at every dawn and winding down at every sunset, solar photons ionize atoms and molecules in the Earth's upper atmosphere. The electron density would build up day after day if there were no efficient means for removing the photoelectrons. This build up would occur not only at Earth but on all of the other planets (except Mercury) and on many of their moons. The most efficient removal mechanism is dissociative recombination (DR) in which an electron is captured by a molecular cation. The identity of the major molecular ions is unique to each planetary ionosphere and moon. At Earth, in the high ionosphere, N_2^+ controls the ionization balance and its DR is described by

$$N_2^+(v) + e^- \rightarrow N + N \quad (1)$$

and by

$$N_2^+(v) + e^- \rightarrow N_2^R \rightarrow N + N, \quad (2)$$

where e^- is an electron, v denotes the vibrational level, N_2^R is a neutral Rydberg state, and the product N atoms can be electronically excited. In two prior papers,[1,2] a theoretical *ab initio* approach is described for determining cross sections and rate constants for $v = 0$[1] and cross sections for $1 \le v \le 4$.[2] Here, rate constants for $1 \le v \le 4$ are reported. CASSCF[3] (Complete Active Space Selfconsistent Field) and CI[4–8] (Configuration Interaction) wave functions are used to determine potential curves, electron capture widths and quantum defects. MQDT[9] (Multichannel Quantum Defect Theory) is used for the calculation of cross sections and rate constants. Details can be found in the prior papers.[1,2] Because the important states that describe the right side of Eq. (1) are diabatic and cross the ion, Rydberg basis functions are not employed and in some cases the most diffuse basis functions are intentionally removed from the bases. The potential curve calculations identify 14 important neutral dissociative states: C-$4^3\Pi_u$, b, 2, $3^1\Pi_u$, $2^1\Sigma_g^+$, $b'^1\Sigma_u^+$, $2^3\Sigma_u^+$, $2^3\Pi_g$, $1^3\Sigma_g^+$, $1^1\Delta_g$, and $2^3\Delta_g$ based upon proximity to the turning points of the lowest 5 ion vibrational levels and to those of vibrationally excited Rydberg levels. The lowest 5 vibrational levels are studied because the electron densities in planetary ionospheres are such that higher levels radiate to $A^2\Pi_u$ long before they undergo DR.

Analysis of the cross sections shows that $2^3\Pi_u$ and $4^3\Pi_u$ are the dominant dissociative routes for $v = 0$ with $C^3\Pi_u$, $3^3\Pi_u$, $2^1\Sigma_g^+$, $b'^1\Sigma_u^+$, and $2^1\Pi_u$ contributing to the structure.[1] The important role of indirect recombination,[10] Eq. (2), is illuminated by showing that the $v = 11$ level of an $n = 3$ Rydberg state causes $C^3\Pi_u$ and $3^3\Pi_u$ to be as important as $2^3\Pi_u$ in a narrow energy region. In addition to Rydberg states having the ground ion core, states having the $A^2\Pi_u$ core also contribute prominently to the cross section structure. For $v = 1$–4, $2^3\Pi_u$ and $4^3\Pi_u$ are dominant routes with some exceptions. In addition to the states that cause structure for $v = 0$, $b^1\Pi_u$, and $2^3\Sigma_u^+$ also contribute. For $v = 2$, the dominant route from 0.0015 to 0.0025 eV is $2^1\Pi_u$. For $v = 3$, $2^3\Sigma_u^+$ is dominant from 0.001 to 0.0025 eV. From 0.001 to 0.002 eV, $2^3\Sigma_u^+$ is dominant for $v = 4$. These nine states are shown in Fig. 1.

In Sec. II, the contributions to the rate constants for $0 \le v \le 4$ are identified and the dominance of the $v = 0$

a)slg@sci.org

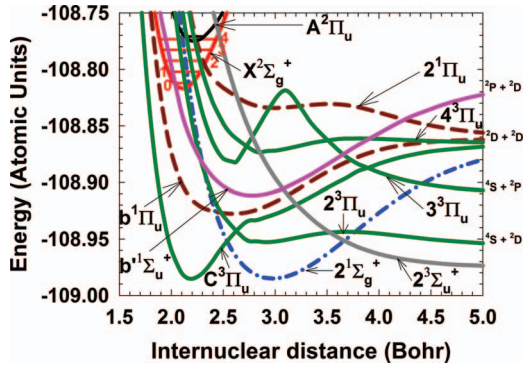

FIG. 1. Potential curves for dissociative routes of N_2 shown with that for the ion ground state, $X^2\Sigma_g^+$ (red) and the first excited state, $A^2\Pi_u$ (upper left, black). The $^3\Pi_u$ (solid, green), $^1\Pi_u$ (brown, dashed), $2^1\Sigma_g^+$ (dash dot, blue), $2^3\Sigma_u^+$ (solid, gray), and $b'^1\Sigma_u^+$ (solid, purple) curves are also shown.

rate constant is shown. Rate constant uncertainties and least squares fits are described in Sec. III. Results are compared to experimental findings and prior theory in Secs. IV and V, respectively. With the derivation of the maximum rate constant, Sec. VI describes how the calculations contribute to the resolution of a more than 30 year old problem in ionospheric modeling. Section VII has the summary and conclusions. Unless noted otherwise, all temperatures are electron temperatures.

II. LEVEL SPECIFIC RATE CONSTANTS

The rate constants are derived from a Maxwellian average over the calculated cross sections.[1,2] The total rate constant for any v is a simple sum of the rate constants for each dissociative symmetry and electron partial wave.

Fig. 2 shows the total DR rate constant for v = 0 and that for each route that contributes more than 10^{-9} cm^3/s to the total. Of the six contributing states, only three cross between or at the turning points for v = 0: $2^3\Pi_u$, $3^3\Pi_u$, and $2^1\Sigma_g^+$. The contribution of $3^3\Pi_u$ is below 10^{-8} cm^3/s because of its small electron capture width.[1] $C^3\Pi_u$ and $2^1\Pi_u$ contribute more than 10^{-9} cm^3/s even though they are over 0.2 a_o outside the

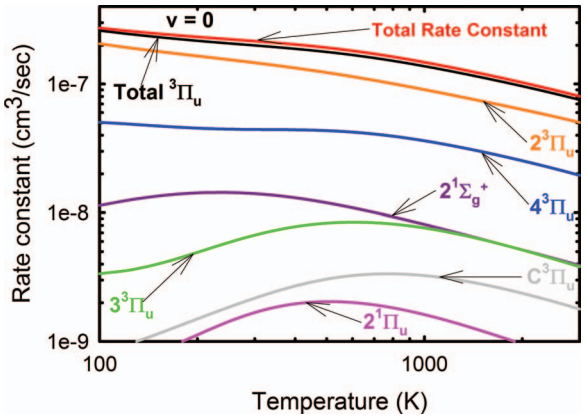

FIG. 2. Rate constants for dissociative routes contributing more than 10^{-9} cm^3/s for v = 0. The total rate constant (red) and the total rate constant due to all the $^3\Pi_u$ routes (black) in addition to $2^3\Pi_u$ (orange), $4^3\Pi_u$ (blue), $2^1\Sigma_g^+$ (dark pink), $3^3\Pi_u$ (green), $C^3\Pi_u$ (gray), and $2^1\Pi_u$ (purple) are shown.

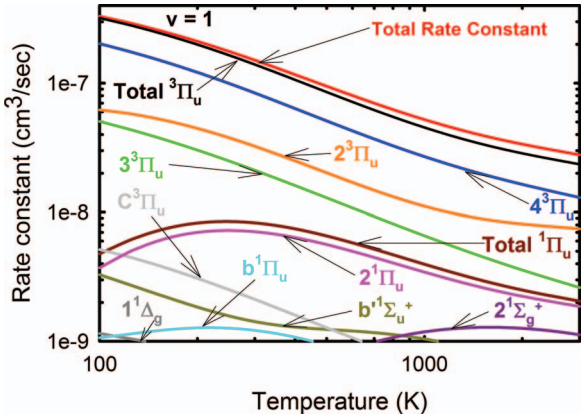

FIG. 3. Same as Figure 2 except rate constants for dissociative routes contributing more than 10^{-9} cm^3/s for v = 1 are shown. The total rate constant for all $^1\Pi_u$ routes (brown) is shown along with $b^1\Pi_u$ (cyan), $b'^1\Sigma_u^+$ (dark yellow), and $1^1\Delta_g$ (dark gray).

v = 0 turning points, demonstrating the importance of indirect recombination (Eq. (2)). The near coincidence of the total $^3\Pi_u$ contribution with that for the total rate constant shows the important role of the $^3\Pi_u$ states. Among these, $2^3\Pi_u$ is the dominant DR route followed by $4^3\Pi_u$. The calculated total rate constant for v = 0 at 300 K is 2.2×10^{-7} cm^3/s and 1.0×10^{-7} cm^3/s at 2005 K.

Compared to Fig. 2, the v = 1 results in Fig. 3 show that the $2^3\Pi_u$ and $4^3\Pi_u$ states have qualitatively swapped positions with the latter state having the dominant contribution at all temperatures. The cause of the swap is clear from Fig. 1 where, at zero electron energy, $2^3\Pi_u$ is near the peak of v = 0 but near the node of v = 1. $4^3\Pi_u$ crosses near the large R turning point of v = 1 but is at about 0.1 a_o beyond the large R turning point of v = 0. The remaining states are the v = 0 contributors with the exception of small contributions from $1^1\Delta_g$, $b^1\Pi_u$, and $b'^1\Sigma_u^+$. The latter state is an open channel at all electron energies from v = 1 but from v = 0, it is only open above 0.1374 eV and leads to $^2P + {}^2D$ atoms. The calculated rate constant at T_e = 300 K is 32 (+12, −7)% below that for v = 0 and 66 (+2, −6)% below at 2005 K (Table II). The uncertainties in these percentages are derived in Sec. III.

For v = 2, Fig. 4 shows that the $^3\Pi_u$ states are the dominant contributors to the cross section with $4^3\Pi_u$ most

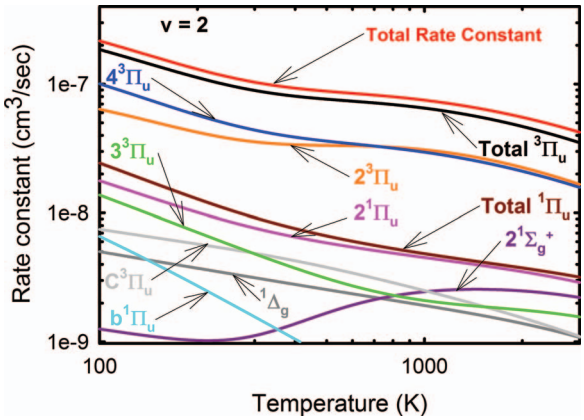

FIG. 4. Same as Figure 3 except rate constants for dissociative routes contributing more than 10^{-9} cm^3/s for v = 2 are shown.

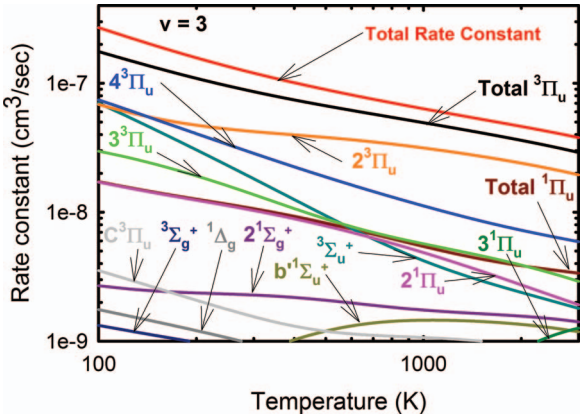

FIG. 5. Same as Figure 4 except rate constants for dissociative routes contributing more than 10^{-9} cm^3/s for v = 3 are shown. The rate constants for $2^3\Sigma_u^+$ (light blue), $1^3\Sigma_g^+$ (dark blue), and $3^1\Pi_u$(dark green) are also shown.

important at low T_e and both $2^3\Pi_u$ and $4^3\Pi_u$ of equal importance at high T_e. At 300 K, the $^3\Pi_u$ states contribute 86% of the total cross section. The $^1\Pi_u$ contribution now exceeds 1.0 $\times$ 10^{-8} cm^3/s at the lowest T_e's. Compared to the v = 0 rate constant, that for v = 2 is 55 (+8, −10)% lower at 300 K and 45 (+3, −10)% lower at 2005 K.

As the vibrational ladder is ascended, the $^3\Pi_u$ states lose dominance as is shown in Fig. 5 for v = 3. At 300 K, the $^3\Pi_u$ states contribute 71% of the total rate constant. A state that did not contribute to v = 0–2 is now apparent, $2^3\Sigma_u^+$. This state makes its greatest contribution at the lowest temperatures constituting 26%, 15%, and 4.7% of the rate constant at 100 K, 300 K, and 3010 K, respectively. Fig. 1 shows that this state comes closer to the large R vibrational turning point as v increases leading to increasing vibrational overlap. The $^1\Pi_u$ contribution is about the same as that for v = 2. The rate constant at 300 K and 2005 K (Table II) is 45 (±15)% and 54 (+4, −10)% respectively, below that for v = 0.

For v = 4, the total $^3\Pi_u$ and $2^3\Sigma_u^+$ contributions are 53% and 27%, respectively, of the total DR rate constant at 300 K. Fig. 6 shows that $4^3\Pi_u$ is the dominant state at all electron temperatures except the lowest where $2^3\Sigma_u^+$ is of comparable magnitude. Compared to lower levels, the $2^3\Pi_u$ contribution

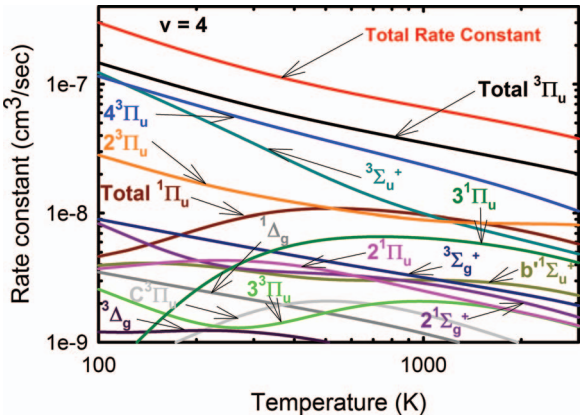

FIG. 6. Same as Figure 5 except rate constants for dissociative routes contributing more than 10^{-9} cm^3/s for v = 4 are shown. The rate constant for $2^3\Delta_g$ (dark purple) is also shown.

is depressed and is exceeded by the total $^1\Pi_u$ rate constant (dominated by $3^1\Pi_u$) for 500 ≤ T_e ≤ 1500 K. $1^3\Sigma_g^+$ and $2^3\Delta_g$ make small contributions to the total rate constant. The total rate constants at 300 K and 2005 K are nearly the same as that for v = 3.

The total rate constants show two trends. First, for excited v above 300 K, especially v = 2, 3, and 4, the rate constants are similar but they are all smaller than that for v = 0. Second, the role of the $^3\Pi_u$ states, while still important, decreases monotonically as v increases. The total numbers of dissociative states with contributions above 1 $\times$ 10^{-9} cm^3/s are 6, 8, 8, 11, and 12 for v = 0, 1, 2, 3, and 4 respectively. The increasing number of dissociative states provides a near uniform sampling of vibrational overlap as v increases. Simultaneously, those states that are important for the DR of the lowest levels become less important as v increases as they are displaced from vibrational peaks and turning points. As these states become less important, they are replaced by new states crossing the high v levels at the large R turning points.

Can these trends be predictive for other molecules? The lowest energy asymptote for N_2^+ DR is N(^{4}S) + N(^{2}D) which lies at 3.4 eV below the ion v = 0. This gap is energetically large enough to allow a repulsive state arising from this asymptote to cross the ion within the v = 0 turning points. The net result is a large DR rate constant from v = 0 with smaller values from higher vibrational levels. A very different situation is found in H_2^+ where the gap between the v = 0 ion and the lowest asymptote participating in DR is only 0.71 eV. (In both H_2^+ and N_2^+, the ground state neutral asymptote does not participate in DR.) This gap is too small to allow a repulsive curve to cross the ion v = 0 within its turning points. Instead the lowest dissociative curve crosses the ion between the v = 0 and v = 1 outer turning points[11] leading to a rate constant from v = 1, 2, and 3 that is 10 times larger[12] than that from v = 0. As new dissociative routes become accessible, the rate constant increases by nearly another factor of 10.[12] Clearly, a detailed knowledge of potential curves and widths is needed before predictions can be made for other molecular ions.

The six states contributing more than 1 $\times$ 10^{-8} cm^3/s to the rate constant for any v and T_e for 100 ≤ T_e ≤ 3000 K are $2^3\Pi_u$, $3^3\Pi_u$, $4^3\Pi_u$, $2^1\Sigma_g^+$, $2^1\Pi_u$, and $2^3\Sigma_u^+$.

The total rate constants for v = 0–2 and v = 0, 3, and 4 are shown in Figs. 7 and 8. The v = 3 and 4 rate constants are nearly identical over the full range of electron temperatures. Remarkably, there is a near coincidence of rate constants for all the *excited* vibrational levels of (0.92–0.82) $\times$ 10^{-7} cm^3/s for 520 < T_e < 610 K where the v = 0 rate constant is about a factor of 2 higher.

III. RATE CONSTANT UNCERTAINTIES AND FITS

In the prior report[1] of the v = 0 rate constant, the uncertainty in the theoretical value is estimated by using a ±15% uncertainty in the calculated widths and ±0.006 a_o in the relative position of the ion and neutral curves. The latter value is taken from the difference between the calculated internuclear distance at which $2^3\Pi_u$ crosses the ion and that for the

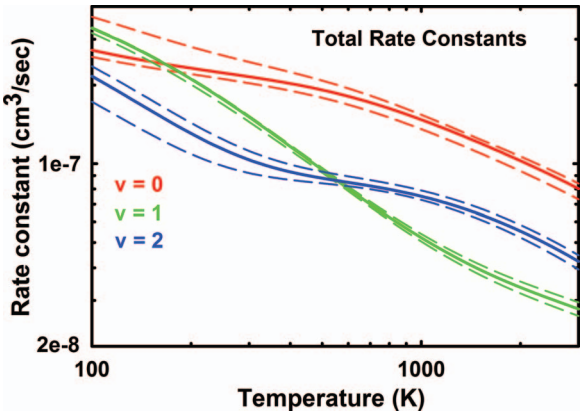

FIG. 7. The total DR rate constants (solid lines) for v = 0 (red), v = 1 (green), and v = 2 (blue) with the upper and lower limit rate constants (dashed lines).

crossing point of an extrapolated experimentally derived potential curve segment of Leoni and Dressler.[13] Here, the uncertainty is improved by eliminating the ion shift of −0.006 a_o and retaining only the +0.006 uncertainty. Since the calculated rate constant uses an ion potential curve that is placed at the experimental equilibrium internuclear separation, R_e, the calculated $2^3\Pi_u$ potential curve is likely to be further from the ion curve than an experimentally derived $2^3\Pi_u$ curve. Although there is no experimentally derived R_e value for $2^3\Pi_u$, the calculated value[1] is likely to be larger than an experimental value. Indeed, this is generally true for calculated diatomic R_e's. The +0.006 a_o uncertainty includes the Leoni and Dressler crossing and puts the $2^3\Pi_u$ curve closer to the ion than the calculated position. The −0.006 a_o uncertainty (i.e., a shift of the repulsive curve away from the ion) is unlikely. For v = 0, the limiting rate constants are calculated from the rate constants arising from the six combinations of an unshifted and shifted ion with the ±15% width uncertainty and the original width. The combinations giving the highest and lowest rate constants are used to determine the upper and lower limit rate constants. These upper and lower limit rate constants are represented by the dashed lines in Figs. 7 and 8. In some cases, different combinations give the extreme rate

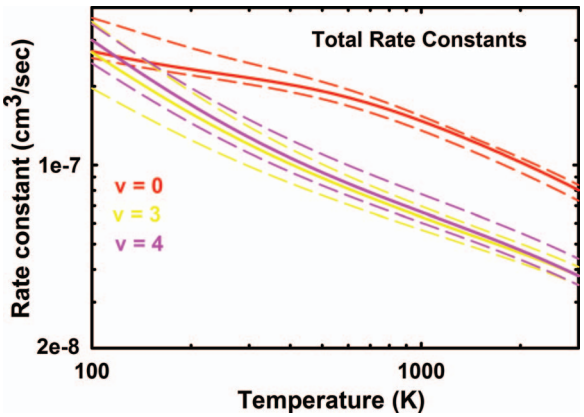

FIG. 8. The total DR rate constants (solid lines) for v = 0 (red), v = 3 (yellow), and v = 4 (purple) with the upper and lower limit rate constants (dashed lines).

constants at different electron energies and this is accounted for in the limiting rate constants.

The calculation of limiting rate constants gives a T_e dependent uncertainty. The upper limit of uncertainty is the difference between the upper limit rate constant and the rate constant calculated without the width or potential curve position uncertainties. The lower limit of uncertainty is the difference between the lower limit rate constant and the rate constant calculated without the width or potential curve position uncertainties. Theoretical uncertainties for DR rate constants have not been reported previously. The width uncertainty and the R shift are applied to the calculated rate constants of all the $^3\Pi_u$ states. For v = 0, only the $^3\Pi_u$ states are used for the uncertainty estimates.

The rate constants have been least squares fitted to the form $a*10^{-7}*(T_e/300)^{-b}$. This form has also been used to represent the upper and lower limit rate constants. The rate constant uncertainties, determined as described above, are also fitted to the same form. The rate constants with the upper and lower limit values and uncertainties are given in Table I. The fits are straight lines if plotted on log-log plots such as those in Figures 2–8. Consequently, they are only approximate representations of the calculated points.[14]

TABLE I. Least squares fits of the calculated rate constants (bold) as a function of electron temperature ($100 < T_e \leq 3000$ K) and ion vibrational level, v, with upper (+) and lower (−) uncertainties and upper (u) and lower limit (ℓ) fits. The rate constants, upper and lower limits and the uncertainties take the form $a \times 10^{-7} \times (T_e/300)^{-b}$.

		α (cm^3/s)[a]	
v		a	b
0		**2.2**	**0.33**
0	+	0.3	1.0
0	−	0.1	0.1
0	u	2.5	0.40
0	ℓ	2.0	0.34
1		**1.5**	**0.79**
1	+	0.0	
1	−	0.1	0.9
1	u	1.5	0.78
1	ℓ	1.4	0.78
2		**1.0**	**0.40**
2	+	0.1	0.8
2	−	0.1	1.0
2	u	1.1	0.42
2	ℓ	0.92	0.31
3		**1.2**	**0.61**
3	+	0.2	1.0
3	−	0.2	1.0
3	u	1.4	0.71
3	ℓ	0.99	0.51
4		**1.3**	**0.65**
4	+	0.2	0.6
4	−	0.2	1.0
4	u	1.5	0.64
4	ℓ	1.1	0.59

[a]Inconsistencies between uncertainties and upper and lower limits are due to round off error.

TABLE II. The calculated rate constants, α (not least squares fitted), at 100 K and 2005 K electron temperature for the lowest 5 ion vibrational levels, v, with the calculated (not least squares fitted) upper and lower uncertainties.

	100 K		2005 K	
v	α (cm^3/s)*	Uncertainty	α (cm^3/s)[a]	Uncertainty
0	2.7	+1.0, −0.1	1.0	+0.0, −0.1
1	3.3	+0.0, −0.1	0.34	±0.02
2	2.2	+0.2, −0.4	0.55	±0.03
3	2.7	+0.8, −0.7	0.46	±0.04
4	3.0	±0.5	0.47	+0.08, −0.04

[a]For the full rate constant, multiply by 10^{-7}.

For v = 0, the total rate constant is $2.2 \times 10^{-7} \times (T_e/300)^{-0.33}$ ($+0.3 \times 10^{-7} \times (T_e/300)^{-1.0}$, $-0.1 \times 10^{-7} \times (T_e/300)^{-0.1}$) cm^3/s for $100 \leq T_e \leq 3000$ K. Note that the uncertainties (in parentheses) are electron temperature dependent. These uncertainties are given for each v in the rows labeled + and −. Also listed are the upper and lower limit fits. In the "a" column, the upper limit of uncertainty is the difference between the value in the u row and the bold value. Similarly, the lower limit of uncertainty in the "a" column is the difference between the bold value and the value in the ℓ row.

The least squares fitted rate constant for v = 0 differs slightly from the prior[1] value of $2.2(+0.4, -0.2) \times 10^{-7} \times (T_e/300)^{-0.40}$ cm^3/s due to the new uncertainty estimate and to the correction of an error in the contribution of the $b'^1\Sigma_u^+$ state to the rate constant. The latter error was present only in the rate constant calculation and not in the reported cross sections.[1,2] For v = 0, the upper and lower limiting rate constant fits are $2.5 \times 10^{-7} \times (T_e/300)^{-0.40}$ cm^3/s and $2.0 \times 10^{-7} \times (T_e/300)^{-0.34}$ cm^3/s for $100 \leq T_e \leq 3000$ K, respectively. Note that these fits are straight lines if plotted on the log-log scales of Figs. 2–8 and they are approximations to the calculated rate constants.

The calculated (not least squares fitted) rate constants at $T_e = 100$ K and 2005 K with the calculated (not least squares fitted) uncertainties are given in Table II. At 100 K, the rate constants are similar except for v = 2, i.e., v = 0, 3 and 4 are within 10% of each other and v = 1 differs from these by at most 22%. Above 300 K, the rate constants for v > 0 are all less than that for v = 0 (see Figs. 7 and 8). At 2005 K, the v = 0 rate constant is about three times that for v = 1 and about two times that for v = 2–4. At 300 K, any experimentally derived rate constant with an upper limit of uncertainty which is below the theoretical lower limit of the v = 0 rate constant, 2.0×10^{-7} cm^3/s, must necessarily be for a plasma that has a substantially excited vibrational population. (Compare the CRYRING distribution discussed below.)

For cases involving thermal equilibrium, the vibrational temperature of the plasma can be determined from the overall DR rate constant measurement.

IV. COMPARISON TO LABORATORY EXPERIMENTS

A partial comparison to experiment was provided previously[1] for the v = 0 rate constant. With the results reported here for vibrationally excited states, a more detailed analysis can now be presented. A review of the early experiments can be found in the volume by Massey and Gilbody[15] and in the article by Biondi.[16] The history of experimental research on the DR of N_2^+ has recently been reviewed by Johnsen.[17] Research on DR of the atmospheric ions has been reviewed by Sheehan and St.-Maurice[18] and by Florescu-Mitchell and Mitchell.[19] Since the proposal[20] that DR of N_2^+ is one of the most important processes in a nitrogen afterglow, experimental techniques dedicated to the study of this reaction have evolved significantly. The early experiments were done in stationary microwave afterglows with pure N_2. The usage of high densities minimized ambipolar diffusion but led to the formation of N_4^+ and gave rate constants that were very large (appropriate for N_4^+ but not N_2^+). Diluting the pure gas with a rare gas and also introducing a mass spectrometer for the identification of the recombining ions significantly improved the technique. The experimental results are compared to the current result in Table III and in Figs. 9 and 10. All the afterglow results in Table III used a rare gas for dilution and a mass spectrometer for ion identification.

A. Stationary afterglows

Kasner and Biondi[23] found a value of 2.9 (±0.3) $\times 10^{-7} cm^3/s$ for $T_e = 300$ K. this value disagrees with that calculated here for v = 0 and disagrees with later values reported by Kasner[24] and Mehr and Biondi[25] (see below).

Kasner[24] reported stationary afterglow results which gave a rate constant of $2.7 \pm 0.3 \times 10^{-7} cm^3/s$ for $205 \text{ K} \leq T_e \leq 480$ K and reported no T_e dependence in this region. The calculated results reported here show a decrease from 2.3 (+0.5, −0.1) to 1.9 (+0.2, −0.1) $\times 10^{-7} cm^3/s$ over this range. The experimental value overlaps the calculated value at 205 K but not at 480 K.

The experiment of Mehr and Biondi[25] gave a rate constant in agreement with the v = 0 value calculated here. The usage of a mass spectrometer alerted the author's to the ever present concentration of N_3^+ and N_4^+ and allowed for the minimization of this problem by reducing the N_2 concentration. But they were not able to entirely eliminate these ions. These ions could have led to an α for N_2^+ that was artificially too high (a difficulty of earlier experiments) but this does not seem to have been the case. Johnsen has commented that the electron energy distribution was likely not entirely Maxwellian.[17] Mehr and Biondi[25] could not account for the difference between their deduced rate constant and those of Kasner[24] and Kasner and Biondi.[23]

The pioneering experiment of Zipf[29] used laser induced fluorescence to measure the individual rate constants, α(v), for DR from the v = 0, 1, and 2 vibrational levels. The individual levels of the ground ion electronic state were pumped to the $B^2\Sigma_u^+$ state. From the time dependence of the intensity of the allowed fluorescence, the population of the ground ion vibrational levels could be followed and the DR rate constant for the lowest 3 vibrational levels could be determined. The experiment assumed that the only sink of excited vibrational levels was DR and ambipolar diffusion. Zipf reported

TABLE III. Comparison to experimental results.

Method[a]	Rate constant (cm^3/s)[b]	T_e (K)	v	Reference
T	2.2 (+[c], −[d]) $(T_e/300)^{-0.33}$	$100 < T_e < 3000$	0	This work
A	2.9 (±0.3)	300 K	0	Kasner and Biondi[23]
A	2.7 (±0.3)	$205 \leq T_e \leq 480$	0	Kasner[24]
A	1.8 (+0.4, −0.2) $(T_e/300)^{-0.39}$	$300 < T_e < 5000$	0	Mehr and Biondi[25]
FA	2.2 (±0.4)	300	0	Mahdavi *et al.*[26]
ST	1.78	300	0	Cunningham and Hobson[27]
MB	1.75 (±0.25)$(T_e/300)^{-0.50}$[e]	$100 < T_e < 25000$	0	Mul and McGowan[28]
A	2.2$(T_e/300)^{-0.39}(T_v/300)^{0.04}$[f]	$300 < T_e < 5000$	...[g]	Zipf (1980)[29]
MB	0.35[h]	300	...[g]	Noren *et al.*[34]
FA	2.0 (±0.4)	300	0	Geoghegan *et al.*[30]
FA	2.6 (±0.4)	300	0	Canosa *et al.*[31]
SR	1.75 (±0.09)$(T_e/300)^{-0.30\pm0.02}$	$80 \leq T_e \leq 1000$	...[i]	Peterson *et al.*[33]
MB	1.50 (±0.23)$(T_e/300)^{-0.39}$	$T_e < 1200$	...[i]	Sheehan and St.-Maurice[18]

[a]T = theory, A = stationary afterglow, FA = flowing afterglow, MB = merged beams, ST = shock tube, and SR = storage ring.
[b]Multiply by 10^{-7}.
[c]$0.3 \times 10^{-7} \times (T_e/300)^{-1.0}$ cm^3/s.
[d]$0.2 \times 10^{-7} \times (T_e/300)^{-0.1}$ cm^3/s.
[e]Corrected for factor of 2 calibration error reported in Refs. 19, 32, and 34.
[f]T_v is the vibrational temperature.
[g]See the discussion in the text.
[h]Estimate from reported cross section.
[i]A high population of vibrationally excited ions was present.

rate constants at 300 K of 2.15, 2.42, and 2.70×10^{-7} cm^3/s for v = 0, 1, and 2, respectively. Although the v = 0 result agrees well with the current work, the trend of increasing α with increasing v is qualitatively in disagreement and outside of the uncertainties calculated here. The source of this disagreement is partially found in the criticism of this experiment by Johnsen[21] who pointed out that in addition to DR and ambipolar diffusion, another reaction was occurring but was neglected in the interpretation, namely ion vibrational change due to collisions with neutral N_2 at 1500 K vibrational temperature. N_2 and N_2^+ have similar fundamental frequencies,[22] 2358 and 2207 cm^{-1}, respectively, so that there is a rapid near resonant collisional vibrational excitation and deexcitation. An additional process neglected by Zipf is vibrational relaxation by electron impact. The relaxation rate constants are of the same order of magnitude as DR rate constants and will be reported separately. Of course, at the time of Zipf's paper, knowledge of the rapidity of this process was nonexistent. The high concentration of neutral N_2 in this experiment compared to the likely electron concentration indicates that ion relaxation collisions with neutral N_2 are probably more important than electron impact relaxation. Indeed, Johnsen pointed out that the time for vibrational change due to collision with N_2 is much shorter than the lifetime of the afterglow.[21] The presence of both processes indicates that the DR contribution to vibrational population loss observed by Zipf was not properly assessed. The formula of Zipf in Table III cannot be used to describe DR. To date, more than 34 years since Zipf's experiment, there are still no experimental determinations of $\alpha(v)$ for v > 0, indicating the difficulty of these measurements. Note that the Mehr and Biondi experiment also suffered the same rapid vibrational change as in Zipf's experiment but the

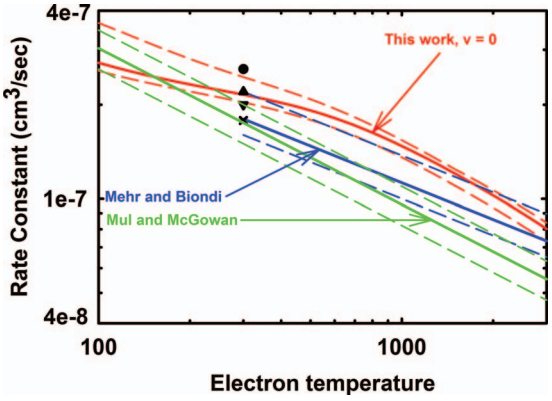

FIG. 9. Experimental and theoretical total rate constants with the limiting uncertainties (dashed lines). The temperature dependent results of Mehr and Biondi[25] (blue) and Mul and McGowan[28] (green) and this work (red) are shown as are the 300 K results of Canosa *et al.*[31] (black, solid circle), Mahdavi *et al.*[26] (black, solid triangle), Geoghegan *et al.*[30] (black, upside down solid triangle), and Cunningham and Hobson[27] (black, cross).

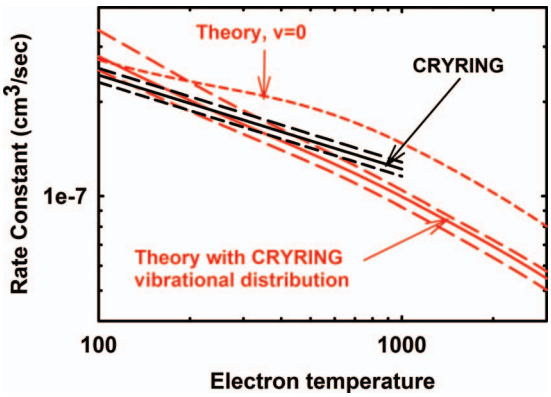

FIG. 10. The CRYRING rate constant (black, solid) shown with the theoretical result for v = 0 (red, short dash) and for the cold CRYRING vibrational distribution (red, solid). The limiting uncertainties are shown with long dashes.

experiment was interpreted as applying to v = 0 which is correct.

Zipf's experiment was reviewed by Bates and Mitchell[35] who derived expressions accounting for the difference between Zipf's deduced DR rate constant and the actual DR rate constant. They deduced an actual DR rate constant for v = 0 from Zipf's data of 2.6×10^{-7} cm^3/s at 300 K and noted the agreement with the result of Canosa *et al.*[31] (see Table III). However, this agreement is only fortuitous. Although their approach is correct, it requires approximations (due to unknown rate constants for several reactions) that give results that do not have quantitative validity. First, electron impact vibrational relaxation is ignored. The importance of this process was not appreciated at the time and the rate constants were unknown. Also due to a lack of data, the rate constants for $N_2^+(v) + N_2(v') \rightarrow N_2^+(v') + N_2(v)$ where $v \neq v'$ were taken to be the same for all $\Delta v = \pm 1$ and ± 2 (where $\Delta v = v' - v$). In the calculation of the actual DR rate constant from v = 0, $\Delta v = \pm 2$ transitions were ignored. The following reaction and its reverse were ignored: $N_2^+(0) + N_2(2) \rightarrow N_2^+(1) + N_2(1)$. For v = 2, in addition to the latter reaction, $\Delta v = \pm 1$ reactions were surprisingly ignored. The value of the resulting actual DR rate constant for v = 2, not given in the paper, is negative.

B. Flowing afterglows

Mahdavi *et al.*[26] determined a rate constant in excellent agreement with the v = 0 value reported here. By moving the recombination region away from the discharge region, the N_2^+ is more likely to collide with cold N_2.

The separation of the discharge and afterglow regions was also used to advantage by the flowing afterglow experiment of Geoghegan *et al.*[30] This experiment also allowed for the neglect of diffusion and gave a rate constant for v = 0 in excellent agreement with that reported here.

Flowing afterglow results were also reported by Canosa *et al.*[31] Although the N_2 densities in their experiment were twice that used by Zipf and 3 times higher than that used by Mehr and Biondi, they claimed that N_4^+ was not a contributor to the measured rate constant. Their result is in excellent agreement with the theory at 300 K.

C. Shock tube

The experiment of Cunningham and Hobson[27] was done in the temperature range 700–2700 K where a $T_e^{-0.37}$ dependence was found in agreement with the dependence found here. The authors reported that the vibrational population was all in v = 0 and that the translational and electronic temperatures were equilibrated. The 300 K value in Table III is their extrapolation of the measurements and is just below the value reported here. Uncertainties were not reported.

D. Multipass merged beams

At the storage ring, CRYRING,[33] the total deduced DR rate constant for ions in an excited vibrational distribution is $\alpha^{CRY} = 1.75\ (\pm 0.09)*10^{-7}*(T_e/300)^{-0.30}$ cm^3/s which is plotted in the paper for $80 \leq T_e \leq 1000$ K and shown here in Fig. 10. As stated above, any reliable experiment giving a DR rate constant (within its range of uncertainty) that is lower than the lower limit of uncertainty on the calculated (not least square fitted) rate constant from v = 0, 2.0×10^{-7} cm^3/s at 300 K, must be observing vibrationally excited N_2^+ if other aspects of the experiment are correct. This observation is consistent with the vibrational distributions found in the CRYRING experiment.[33] However, a common misconception among those who quote the CRYRING[33] paper is that the vibrational population of the ions was determined. This is not the case. Only the product of the relative population and the relative rate constant for each v was derived for zero energy electrons. The relative vibrational population follows only if the DR rate constants are independent of v. In the CRYRING study, two ion sources generating different ion vibrational populations were used. The total rate constants from the two sources were found to be similar. This led to the conclusion that "...the rates cannot be strongly dependent upon the vibrational quantum number."[33] Is this conclusion valid? In a prior paper, theoretically determined "flattened" rate constants (see Figure 12 in Ref. 2) were calculated for electron energies between 0.001 and 1.0 eV. These rate constants are a function of energy, not temperature, and are for storage ring electron beams which are characterized by different temperatures in directions parallel and perpendicular to the beam direction. Theory showed that these rate constants are approximately independent of v at the lowest energy, 0.001 eV, but diverge from v independence at higher energies. At CRYRING, the product of relative ion vibrational population and level specific relative rate constant was measured at "zero" eV. Because theory shows that at low energy the rate constants are approximately independent of v, the vibrational populations can be deduced from the measured products. The colder CRYRING ion source (for which the rate constant is quoted above) had a vibrational population of 46%, 27%, 10%, and 16% for v = 0, 1, 2, and 3, respectively, while that of the hotter source was 30%, 31%, 19%, and 18%. Experimental uncertainties for the product of the relative population and the level relative rate constant were not reported. Combining the vibrational level specific theoretical rate constants with these populations gives a least squares fit total rate constant for the cold source of $1.7 \times 10^{-7} \times (T_e/300)^{-0.45}$ $(+0.2 \times 10^{-7} \times (T_e/300)^{-1.1}, -0.1 \times 10^{-7} \times (T_e/300)^{-0.54})$ cm^3/s for $100 \leq T_e \leq 3000$ K and $1.5 \times 10^{-7} \times (T_e/300)^{-0.50}$ $(+0.2 \times 10^{-7} \times (T_e/300)^{-1.1}, -0.1 \times 10^{-7} \times (T_e/300)^{-0.73})$ cm^3/s for the hot source. The cold source rate constant is in very good agreement with the cold source CRYRING rate constant quoted above. The hot source rate constant is below that for the cold source in agreement with the CRYRING measurements. An experimental hot source rate constant fit was not reported. The rate constants are compared in Fig. 10 which shows the theoretical raw data (not a fit) with the experimental fit[33] quoted above (straight line). These total rate constants overlap up to 600 K even though the theoretical v = 0 specific rate constant is quite different from those for v > 0 at and above 300 K (See Sec. II). The v = 0 rate constant from this work is also shown because of the slope difference between

the two results. The CRYRING rate constant has a slope that is close to that of the v = 0 theory result.

The CRYRING assumption of rate constant similarity[33] for all v is not valid above room temperature as illustrated in Figs. 7 and 8 and discussed in Sec. II (with the exception of the v = 3 and v = 4 rate constants which overlap at all temperatures). At 2005 K, the theoretical v = 0 rate constant exceeds that for v = 1, 2, 3 and 4 by factors of 2.9 (+0.2, −0.4), 1.8 (+0.1, −0.3), 2.2 (+0.2, −0.4), and 2.1 (+0.2, −0.5), respectively.

Because of the difference in the deduced product of relative population and rate constant for v = 2 and v = 3, it was speculated[33] that the rate constant for v = 2 is less than that for v = 3 at zero electron energy. At 100 K electron temperature, the uncertainties in the rate constants are too large for the theory to identify the larger rate constant. For 800 ≤ T_e ≤ 2400 K, the rate constant for v = 2 is greater than that for v = 3.

E. Single pass merged beams

Mul and McGowan,[28] using the MEIBE apparatus, found a rate constant that falls below the theory above 300 K (Fig. 9) indicating the possible presence of vibrationally excited ions. They found a T_e dependence of −0.5 for not only N_2^+ but also O_2^+ and NO^+. This finding is unreasonable since the slopes of the dissociative curves and the positions of resonances, all contributing to the T_e dependence, differ among these three ions.

Additional work with the MEIBE apparatus[34] gave a cross section that was a factor of 5 lower than the results of Mul and McGowan.[28] Rate constants were not reported. Cross sections were obtained under conditions that were thought to apply to N_2^+ ions in the ground electronic and vibrational state. Under other conditions thought to generate excited N_2^+, the cross sections were comparable to those reported from the prior MEIBE experiment. The authors concluded that excited N_2^+ has much higher cross sections than the v = 0 ground state. However, the electronic and vibrational distribution of the excited N_2^+ was not characterized. These results are contrary to those found here. The factor of 5 decrease in the v = 0 rate constant is outside of the uncertainties calculated here and cannot be correct. Furthermore, if the excited N_2^+ was not electronically excited but only vibrationally excited, the results are qualitatively different from those found here and also cannot be correct.

This second MEIBE experiment was criticized by Bates and Mitchell[35] who pointed out that if $\alpha(0)$ is 5 times lower than all prior values, $\alpha(1)$ would have to be 1.8×10^{-6} cm^3/s. In support of their conclusion, as shown below in Sec. VI, a value of 1.8×10^{-6} cm^3/s exceeds the maximum allowed value and is not possible.

Sheehan and St.-Maurice[18] reported the third MEIBE experiment on N_2^+. They claimed that the CRYRING rate constant is incorrect because their deduced cross section is similar to the CRYRING result but their rate constant is lower, 1.5×10^{-7} cm^3/s at 300 K. They recalculated the CRYRING rate constant and obtained a value identical to their rate constant at 300 K. I have recalculated the CRYRING rate constant for 80 < T_e < 1000 K from the CRYRING cross section data and get a value of $1.73 \times 10^{-7} \times (T_e/300)^{-0.27}$ cm^3/s, essentially in agreement with the CRYRING result. The range of T_e used for the published fit was not given in the CRYRING paper and may account for the small difference. The recalculation of the CRYRING rate constant reported here indicates that the Sheehan and St.-Maurice rate constant given in their paper and in Table III is not correct and that their correct rate constant agrees with the CRYRING rate constant. This is unusual since the agreement indicates that both experiments may have had the same excited vibrational distribution.

V. COMPARISON TO OTHER THEORY

Besides the earlier results reported from this laboratory, there have been only two prior theoretical calculations of N_2^+ DR rate constants. The pioneering calculations of Michels[36] have been summarized previously.[1] A very recent report[37] by Fifirig of an MQDT calculation of rate constants and cross sections for the lowest 4 ion vibrational levels uses potential curves, widths and quantum defects previously calculated in this laboratory for the $^3\Pi_u$[1] and $^1\Sigma_g^+$[41] symmetries. The $^1\Sigma_u^+$ symmetry is also included with data coming from Spelsberg and Meyer.[38] Excited core Rydberg states are included for $^3\Pi_u$ and $^1\Sigma_g^+$ compared to the calculations reported here where they were included for $^3\Pi_u$, $^1\Sigma_g^+$, $^1\Pi_u$, and $^1\Sigma_u^+$.[1] Fourteen dissociative states are included here and 6 are included by Fifirig. An integration grid of 0.01 a_o is used for the vibrational wave functions between 0.5 and 25 a_o compared to a grid of 0.001 a_o used here between 1.0 and 8.0 a_o.

The remaining significant differences involve the K matrix and the ion potential curves. Fifirig's K matrix includes the calculation of the elements, $K_{dd'}$, but she did not report the values. These matrix elements are set to zero here based upon the prior argument[9] that they are negligible. For the ground ion state, Fifirig uses an RKR curve from Morioka *et al.*[39] and an *ab initio* curve of Bing and Wei[40] for the $A^2\Pi_u$ state. In the calculations reported here, an RKR[22] curve is used for the lower part of the $X^2\Sigma_g^+$ well, supplemented with *ab initio* points for the remainder of the well.[41] An *ab initio* curve is used for $A^2\Pi_u$.[41] Twenty three vibrational levels are included here in both the $X^2\Sigma_g^+$ and $A^2\Pi_u$ potential wells as well as in the Rydberg wells.[2] This covers all the Rydberg vibrational levels with the X and A cores that are present at energies up to 1 eV above any level up to v = 4 of $X^2\Sigma_g^+$. Because the MQDT approach has a closure condition over the vibrational levels (see Eqs. (15) and (16) of Ref. 9), tests were done to determine the effect of additional vibrational levels. They have only a negligible effect and further expansion of the vibrational basis is ignored. The usage of the RKR curve of Morioka *et al.*, allows Fifirig to use 77 vibrational levels in the $X^2\Sigma_g^+$ curve. The *ab initio* curve of Bing and Wei is determined using a very similar approach to that used here and the spectroscopic constants are very similar. The potential curve is determined out to 7.6 a_o, quite distant from Fifirig's outer limit of integration at 25 a_o. Fifirig uses 71 vibrational levels in the $A^2\Pi_u$ potential.

Fifirig describes the small interaction between the direct and indirect processes in the prior calculation[41] of the DR cross section along the $2^1\Sigma_g^+$ channel as due to the presence of only "... a small part of the closed ionization channels." In the case of the indirect mechanism involving the ground core Rydbergs, this is due to the very small electronic width and is not connected to the size of the vibrational basis that was used. The larger width for the Rydbergs having the $A^2\Pi_u$ core clearly leads to an enhanced role for the indirect mechanism (compare Figs. 2 and 3 of Ref. 41).

A comparison of cross sections shows disagreement between those reported earlier[1,2] and those of Fifirig.[37] Some disagreement is to be expected since several of the less important states (not included by Fifirig) and discussed previously,[1,2] contribute to structure in the cross sections but do not play a significant role in determining the rate constants. However, her cross sections are generally lower than those obtained in this laboratory. The v = 0 cross section at 0.001 eV is 2×10^{-13} cm^2 compared to that of 3×10^{-13} cm^2 found here. The n = 8, v = 1 ground core $^3\Pi_u$ resonance which was found near 0.009 eV is absent in her total cross section. A small dip in her cross section near 0.006 eV is absent in the prior report of the cross section used here.[1] For v = 0, the Fifirig cross section is mostly below the CRYRING cross section below 0.07 eV (see Fifirig's Fig. 6) but the calculated rate constant at 300 K is above the CRYRING rate constant, indicating that there may be an error in Fifirig's calculations. For v = 1, both results show that the cross sections at 0.001 eV are larger than those for v = 0 and both have a similar drop above threshold indicating the presence of a threshold resonance. However, the n = 8, v = 2 and n = 4 v = 6 $^3\Pi_u$ ground core resonances which are prominent[2] have only a narrow peak in the full cross section and disappear in Fifirig's ground core cross section. A large drop in the cross section near 0.04 eV is present in both cross sections. For v = 2, the cross section reported previously[2] is 1×10^{-13} cm^2 at 0.001 eV and falls slightly as the electron energy increases followed by a rise to a local peak near 0.0035 eV due to $^3\Pi_u$ resonances. The Fifirig cross section is 6×10^{-14} cm^2 at 0.001 eV and falls as the energy increases to 0.007 eV without showing a peak near 0.0035 eV. For v = 3, the cross section reported previously[2] is larger than Fifirig's at low energy.

Although there is agreement between the 300 K rate constants reported here and the values of Fifirig, there appears to be an error in her paper as pointed out in the prior paragraph. The cross sections for v = 0 reported in her paper give a room temperature rate constant of 0.8×10^{-7}cm^3/s instead of the reported[37] value of 2.1×10^{-7} cm^3/s.

DR rate constants are sensitive to the value of the crossing point of ion and dissociative curves and to the slope at the crossing point. The crossing point of the $2^3\Pi_u$ and $X^2\Sigma_g^+$ curves calculated here comes at 2.136 a_o. Shifting the $^3\Pi_u$ potential curves (for the calculation of uncertainties) shows that the 300 K v = 0 rate constant increases as the crossing point moves to smaller R from 2.136 a_o and decreases as the crossing point moves to larger R. A comparison with other curves in the literature can therefore lead to predictions of rate constants that would be derived with these curves assuming other inputs are the same (e.g., widths and quantum defects). Potential curves and quantum defects for N_2 are reported by Little and Tennyson[42] using the R matrix approach. The potential curves (see Fig. 8 in Ref. 42) are adiabatic and do not cross the ion. They plot the $^3\Pi_u$ curves used here with their curves and with the diabatic curves of Hochlaf *et al.*[43] In the case of adiabatic curves, one can only estimate where diabatic curves based upon the adiabatic curves would cross the ion. Visual inspection shows that all the $^3\Pi_u$ curves have similar slopes to that found here. Visual inspection also indicates that the R matrix derived $2^3\Pi_u$ curve is likely to cross the ion at a slightly greater R than that calculated here and that of Hochlaf *et al.* crosses the ion at a still greater R. Usage of these curves in the approach used here would lead to slightly smaller v = 0 rate constants at 300 K. The crossing points of the $3^3\Pi_u$ and $4^3\Pi_u$ curves are considerably larger than that found here. In the calculations reported here a large CI (configuration interaction) wave function in addition to CASSCF for the orbitals is used. However, in the R matrix calculations only a CASSCF is used. In the Hochlaf *et al.* calculations, the approach is similar to that used here with the exception that a more diffuse basis is used allowing for the description of Rydberg character. Diffuse basis functions are intentionally omitted from the calculations reported here in order to describe diabatic valence dissociative states. This difference may account for the difference in crossing point values.

In the R matrix calculations,[42] a single basis, cc-pVQZ, is used for both the valence and Rydberg states. In the formulation of this basis,[44] the diffuse s and p exponents are determined[44] so as to provide an improved description of the outer parts of valence orbitals and the diffuse d, f, and g Gaussians describe the polarization of valence orbitals. Although Little and Tennyson calculate quantum defects with this basis, it is not appropriate for Rydberg orbitals. For example, the most diffuse s, p, and d Gaussian primitives in this basis have exponents of 0.1552, 0.1428, and 0.335, respectively.[44] But the tightest exponents needed to describe n = 3 orbitals in the Rydberg basis sets of Kaufmann *et al.*[45] are 0.00588 and 0.009988 for s and p Rydbergs and 0.00492 for n = 4 d Rydbergs. Therefore, in the R matrix approach, contrary to the statement in the paper, the Rydberg description cannot be coming from the cc-pVQZ basis but appears to arise from the continuum aspects of the calculation (possibly the Gaussian fits to Bessel functions). Inspection of the quantum defects in Tables 3–7 of Ref. 42 shows that many of the defects are calculated for high n where they are not converged with respect to n. It is not possible to know whether the lack of convergence is due to a poor description of the Rydberg space or to interactions between neighboring Rydberg states of the same symmetry.

Quantum defects are an essential component in the calculation of DR rate constants. The defects determine both the energies of the intermediate Rydberg states of Eq. (2) and the probability of electron capture into those states. Tables IV and V have quantum defects (for the $X^2\Sigma_g^+$ and $A^2\Pi_u$ core) for all the relevant DR symmetries along with the results of Cremaschi[46] and Little and Tennyson.[42] In the results reported here, cc-pVTZ[44] and cc-pVQZ[44] basis sets are used for the valence states and separate calculations with large diffuse Rydberg basis sets[45] are done for the Rydberg

TABLE IV. Quantum defects, μ, for principal quantum number, n, and Rydbergs having the $X^2\Sigma_g^+$ core.

	μ(n)			
Rydberg symmetry	This work	Cremaschi *et al.*[46]	Little and Tennyson[42]	Experiment[a]
$^3\Pi_u$, $p\pi_u$	0.7450(3)[1]	0.67(3)	0.739(3)	0.75(3)[47]
$^1\Sigma_g^+$, $s\sigma_g$	0.9368(10)	0.92(3)	0.857(8)	0.98(3)[22]
$^1\Sigma_g^+$, $d\sigma_g$	0.1096(10)[41]	0.10(3)	0.119(7)	0.171(3)[48]
$^1\Sigma_u^+$, $p\sigma_u$	0.5627(11)	0.50(6)	0.626(11)	0.60822(∞)[49]
$^1\Pi_u$, $p\pi_u$	0.7372(3)	0.66(3)	0.668(3)	0.68375(∞)[49]
$^1\Delta_g$, $d\delta_g$	− 0.0065(6)	− 0.03(6)	− 0.008(8)	
$^3\Sigma_g^+$, $s\sigma_g$	1.005(10)	0.92(5)	1.156(7)	1.08(3)[22]
$^3\Sigma_g^+$, $d\sigma_g$	0.0184(9)	0.11(4)	0.008(6)	
$^3\Sigma_u^+$, $p\sigma_u$	0.5890(11)	0.57(6)	0.776(5)	0.77(3)[22]
$^3\Pi_g$, $d\pi_g$	− 0.0494(9)	− 0.14(6)	− 0.051(7)	
$^3\Delta_g$, $d\delta_g$	− 0.0035(6)	− 0.03(6)	0.020(6)	

[a]The comparison with theory is approximate since the experimental quantum defects are derived from the difference between the v = 0 energies of the ion X state and the state of interest whereas the theoretical values are R dependent. Those calculated here are for R = 2.1602 a_o. Those in column 3 are for 2.10973 a_o (the experimental R_e of $X^2\Sigma_g^+$).

states. Contrary to the statement in the paper by Little and Tennyson,[42] "average" quantum defects are not determined here. Instead the quantum defects are calculated for each reported n for a range of R and some have been described previously.[1] Table IV shows that in spite of the inadequacy of the bound Rydberg basis, the R matrix quantum defects are mostly in surprisingly good agreement with those calculated here and those calculated by Cremaschi.[46] For the important $^3\Pi_u$ symmetry, the defect calculated here agrees with the R matrix result and is slightly closer to the experimentally derived value. Because the R matrix calculations use several ion target states, interactions between Rydberg series having different ion cores and free electron partial waves are included. This means that the R matrix quantum defects cannot be used in a DR cross section calculation requiring individual electron partial waves unless the mixing of the partial waves is included.

An example of a disagreement among the different treatments is for $^3\Sigma_u^+$ where good agreement is found between the defect calculated here and that found by Cremaschi *et al.* but both differ from that found in the R matrix approach. Both the Cremaschi *et al.* defect and that calculated here and given in Table IV use a single $p\sigma_u$ partial wave coupled to the $X^2\Sigma_g^+$ ground state. However, Cremaschi *et al.* also reported a defect of 0.74 in which this state is mixed with other channels. This defect is in agreement with the R matrix result. The additional channels may have included $A^2\Pi_u$, $p\pi_g$ and $B^2\Sigma_u^+$, $s\sigma_g$.

TABLE V. Quantum defects, μ, for principal quantum number, n, and Rydbergs having the $A^2\Pi_u$ core.

	μ(n)			
Rydberg symmetry	This work	Cremaschi *et al.*[46]	Little and Tennyson[42]	Experiment[a]
$^3\Pi_u$, $s\sigma_g$	1.009(10)[1]	1.01(3)	1.022(3)	1.086045(3)[50]
$^1\Sigma_g^+$, $p\pi_u$	0.5593(10)[41]	0.65(3)	0.634(3)	
$^1\Sigma_u^+$, $d\pi_g$	− 0.05232(9)	− 0.11(3)		
$^1\Pi_u$, $s\sigma_g$	0.9966(10)	0.98(3)	0.172(3)	1.05385(3)[22]

[a]The comparison with theory is approximate since the experimental quantum defects are derived from the difference between the v = 0 energies of the ion A state and the state of interest whereas the theoretical values are R dependent. Those calculated here (in column 2) are for R = 2.1531 a_o. Those in column 3 are for R = 2.10973 a_o (the experimental R_e of $X^2\Sigma_g^+$).

Quantum defects for Rydbergs having the $A^2\Pi_u$ core (see Table V) agree with those of Cremaschi *et al.* and Little and Tennyson except for $^1\Pi_u$, $s\sigma_g$ where the defect calculated here, that of Cremaschi *et al.* and the experimentally derived value are about a factor of six larger than that of Little and Tennyson.

VI. IONOSPHERIC MODELS AND MAXIMUM RATE CONSTANT

The variation of the DR rate constant with v has been a topic of great interest to aeronomy for more than 30 years. During this time, there was no satisfactory explanation for the factor of two discrepancy between the satellite measurements of the N_2^+ ionospheric density and the model densities. It was proposed[51] that this discrepancy could be resolved in the models if the rate constant for N_2^+ DR for v > 0 was between a factor of 21 and 35 greater than that for v = 0 or if the rate constants from v = 2, 3, and 4 were zero and that for v = 1 was 23 times greater than that for v = 0. In both cases, the optimal v = 0 rate constant was found to be 0.8×10^{-7} cm^3/s, about 46% below the value calculated here at an ionospheric electron temperature of 1000 K. Are these high values for excited v rate constants physically possible? The DR rate constant along dissociative route, d, from vibrational level, v, and for capture of a single electron partial wave is given by[9]

$$\sigma_{dv} = \frac{\hbar^2 \pi r}{4m\varepsilon} |S_{dv}|^2,$$

where r is the ratio of multiplicities of the dissociative and ion states, m is the electron mass, ε is the electron energy, and S_{dv} is an element of the scattering matrix. The maximum value for σ_{dv} is obtained by setting $S_{dv} = 1$. For the $^3\Pi_u$ capture symmetry and the $^2\Sigma_g^+$ ion, r = 3 and only a single partial wave, $\ell = 1$, is important. The maximum cross section is given by

$$\sigma_{dv}^{max} = \left(\frac{0.60\,r \times 10^{-15}}{\varepsilon} \right) cm^2, \quad (3)$$

where the units of ε are eV. The maximum value of the Maxwellian spherically averaged rate constant is

$$\alpha_{dv}^{max}(Te) = \sqrt{\frac{8}{\pi m k^3 T_e^3}} \int_0^\infty \sigma_{dv}^{max} e^{\frac{-\varepsilon}{kT_e}} \varepsilon d\varepsilon. \quad (4)$$

where k is the Boltzmann constant. Substituting (3) into (4) gives

$$\alpha_{dv}^{max}(T_e) = 4.3 \times 10^{-6} r T_e^{-\frac{1}{2}} cm^3/s.$$

Inserting r yields $\alpha_{dv}^{max}(1000\,K) = 4.1 \times 10^{-7} cm^3/s$. This calculated maximum value shows that both scenarios are rigorously impossible. Our calculated rate constants for v > 0 are smaller than that for v = 0 at all electron temperatures (except below 170 K). Biondi[52] criticized the proposals and our results support that criticism. The results are also

compatible with and support those first reported by Richards[53] who recently contributed to the resolution of the factor of 2 problem by using an improved rate constant[54] for $O^+(^2D) + N_2$ in the model.

VII. SUMMARY AND CONCLUSIONS

A thorough study has been completed of the DR rate constants for the lowest 5 vibrational levels of the ion ground state and for $100 \leq T_e \leq 3000$ K. Fourteen dissociative states over nine electronic symmetries (describing the right side of Eqs. (1) and (2)) were included in the calculations. Two of the symmetries ($^1\Sigma_g^+$ and $^3\Sigma_g^+$) used two partial waves for the electrons generating eleven Rydberg series for each of the included 23 vibrational levels of the ion ground state. For the Rydberg states having the $A^2\Pi_u$ core, a single partial wave is included for each dissociative symmetry and 4 Rydberg series are included for each of the 23 vibrational levels included in the A core. A total of $23 \times (11 + 4) = 345$ Rydberg series are included for the intermediate states labeled N_2^R in Eq. (2).[55] The results show that six dissociative states over four electronic symmetries contribute more than 1×10^{-8} cm^3/s to the rate constant for one or more vibrational levels: $2^3\Pi_u$, $3^3\Pi_u$, $4^3\Pi_u$, $2^1\Sigma_g^+$, $2^1\Pi_u$, and $2^3\Sigma_u^+$.

For v = 0, the dominant dissociative channel is $2^3\Pi_u$ followed by $4^3\Pi_u$. For v = 1, the order of importance is reversed. $4^3\Pi_u$ dominates the v = 2 rate constant at low temperatures but both 2 and $4^3\Pi_u$ are dominant at high temperatures. The $^3\Pi_u$ states are less dominant for v = 3 than for the lower levels. $2^3\Pi_u$ is dominant at most temperatures followed by $4^3\Pi_u$ and $1^3\Sigma_u^+$ below 500 K. $^3\Pi_u$ states contribute only about half of the total rate constant at 300 K for v = 4 with the remainder coming from $1^3\Sigma_u^+$ and $3^1\Pi_u$.

The relative values of the vibrational level specific rate constants undergo a qualitative change with increasing electron temperature. At 100 K, with the exception of v = 2, all the rate constants overlap within the uncertainties. At 300 K, the v = 1, 2, 3, and 4 total rate constants are 32%, 55%, 45%, and 41% respectively below that for v = 0 with the v = 0 dominance remaining at higher temperatures.

The rate constant calculated here for v = 0 is in excellent agreement with many of the prior afterglow results.

At low temperatures, the calculated rate constants agree qualitatively with the CRYRING conclusion that the rate constants are v independent. This agreement disappears above 300 K where the theoretical rate constant for v = 0 significantly exceeds that those for v > 0. The calculations show that any experiment reporting a rate constant at 300 K which is below the calculated (not fitted) lower limit of uncertainty for the theoretical v = 0 rate constant, 2.0×10^{-7} cm^3/s, is likely to involve a substantial population of vibrationally excited ions.

To date, there are no experimental determinations of rate constants for excited v. The CRYRING[33] experiment reported the products of vibrational population and vibrational level specific rate constants for v = 0–3 at "zero" electron energy. With the CRYRING products for the cold and hot ion sources in conjunction with the theoretical vibrational level specific rate constants (which are not the same for all v) total rate constants are calculated. That for the cold source is in very good agreement with the reported CRYRING cold source total rate constant. For the hot source, the numerical experimental rate constant was not reported but the calculated rate constant is less than and similar to that for the cold source in agreement with the experimental findings. Rate constant v independence is not needed to derive similar total rates from two different ion population distributions.

The rate constant reported by Sheehan and St.-Maurice[18] is not consistent with the reported cross section. Contrary to the statement in their paper, their rate constant agrees with the CRYRING[33] rate constant.

Comparisons with R matrix calculations[42] and with calculations of Hochlaf *et al.*[43] show qualitative agreement for the $^3\Pi_u$ potential curves. For the quantum defects, there is good general agreement with the R matrix[42] and Cremaschi *et al.*[46] results. However, for the A core $^1\Pi_u$, $s\sigma_g$ Rydberg series, the R matrix[42] quantum defect differs by a factor of 6 from that calculated here and that calculated by Cremaschi *et al.*[46]

The only prior theoretical calculation[37] of vibrational level specific rate constants used much of the data calculated here but reported MQDT rate constants that are not consistent with the reported cross sections.

Since the DR rate constants for excited v are all smaller than that for v = 0 (except at the lowest temperatures which are not relevant to ionospheric models), the theory reported here contributes to the resolution of a long standing problem concerning the N_2^+ ionospheric abundance.

In spite of the recent advances in the experimental measurements of DR rate constants, there is a clear lack of data for vibrationally excited levels. The only experimental data in the literature is that for H_2^+ and D_2^+.[12] It is hoped that the detailed calculations reported here will inspire the development of new techniques for the laboratory determination of DR rate constants of specific vibrationally excited ion levels.

ACKNOWLEDGMENTS

This research is supported by the National Science Foundation under Grant No. ATM-0838061 and by NASA under Grant Nos. NNX14AC61G and NNX14AJ41G.

[1] S. L. Guberman, J. Chem. Phys. **137**, 074309 (2012).
[2] S. L. Guberman, J. Chem. Phys. **139**, 124318 (2013).
[3] H.-J. Werner and P. J. Knowles, J. Chem. Phys. **82**, 5053 (1985).
[4] P. E. M. Siegbahn, A. Heilberg, B. Roos, and B. Levy, Phys. Scr. **21**, 323 (1980).
[5] P. E. M. Siegbahn, J. Chem. Phys. **72**, 1647 (1980).
[6] P. E. M. Siegbahn, C. W. Bauschlicher, B. Roos, P. R. Taylor, J. Almlöf, Molecule-Sweden.
[7] H.-J. Werner and P. J. Knowles, J. Chem. Phys. **89**, 5803 (1988).
[8] H.-J. Werner, P. J. Knowles, R. Lindh, F. R. Manby, M. Schütz *et al.*, MOLPRO, version 2000.1, a package of *ab initio* programs, 2000, see http://www.molpro.net.
[9] S. L. Guberman and A. Giusti-Suzor, J. Chem. Phys. **95**, 2602 (1991).
[10] J. N. Bardsley, J. Phys. B **1**, 365 (1968).
[11] S. L. Guberman, J. Chem. Phys. **78**, 1404 (1983).
[12] S. Krohn, H. Kreckel, L. Lammich, M. Lange, J. Levin, D. Schwalm, D. Strasser, R. Wester, A. Wolf, and D. Zajfman, *Electron Induced Vibrational Deexcitation of the Molecular Ions* H_2^+ *and* D_2^+ *in Dissociative Recombination of Molecular Ions with Electrons*, edited by S. L. Guberman (Kluwer Academic, New York, 2003), p. 127; S. Krohn, Z. Amitay, A. Baer,

D. Zajfman, M. Lange, M. Knoll, J. Levin, D. Schwalm, R. Wester, and A. Wolf, Phys. Rev. A **62**, 032713 (2000).
[13]M. Leoni and K. Dressler, J. Appl. Math. Phys. **22**, 795 (1971).
[14]See supplementary material at http://dx.doi.org/10.1063/1.4901892 for the calculated rate constants.
[15]H. S. W. Massey and H. B. Gilbody, *Electronic and Ionic Impact Phenomena* (Clarendon Press, Oxford, 1974), vol. IV.
[16]M. A. Biondi, "Dissociative recombination of electrons and ions: The early experiments," in *Dissociative Recombination of Molecular Ions with Electrons*, edited by S. L. Guberman (Kluwer Academic, New York, 2003), p. 13.
[17]R. Johnsen, "DR experiments in the 60 years since the Bates paper," J. Phys. Conf. Ser. **300**, 012002 (2011).
[18]C. H. Sheehan and J.-P. St. -Maurice, J. Geophys. Res. **109**, A03302, doi:10.1029/2003JA010132 (2004).
[19]A. I. Florescu-Mitchell and J. B. A. Mitchell, Phys. Rep. **430**, 277 (2006).
[20]J. Kaplan, Phys. Rev. **73**, 494 (1948).
[21]R. Johnsen, Int. J. Mass Spectrom. Ion Processes **81**, 67 (1987).
[22]A. Lofthus and P. H. Krupenie, J. Phys. Chem. Ref. Data **6**, 113 (1977).
[23]W. H. Kasner and M. A. Biondi, Phys. Rev. **137**, A317 (1965).
[24]W. H. Kasner, Phys. Rev. **164**, 194 (1967).
[25]F. Mehr and M. A. Biondi, Phys. Rev. **181**, 264 (1969).
[26]M. R. Mahdavi, J. B. Hasted, and M. M. Nakshbandi, J. Phys. B **4**, 1726 (1971).
[27]A. J. Cunningham and R. M. Hobson, J. Phys. B **5**, 2328 (1972).
[28]P. M. Mul and J. Wm. McGowan, J. Phys. B **12**, 1591 (1979).
[29]E. C. Zipf, Geophys. Res. Lett. **7**, 645, doi:10.1029/GL007i009p00645 (1980).
[30]M. Geoghegan, N. G. Adams, and D. Smith, J. Phys. B **24**, 2589 (1991).
[31]A. Canosa,, J. C. Gomet, B. R. Rowe, and J. L. Queffelec, J. Chem. Phys. **94**, 7159 (1991).
[32]J. B. A. Mitchell, Phys. Rep. **186**, 215 (1990).
[33]J. Peterson, A. Le Padellec, H. Danared, G. H. Dunn, M. Larsson, Å. Larson, R. Peverall, C. Strömholm, S. Rosén, M. af Ugglas, and W. J. van der Zande, J. Chem. Phys. **108**, 1978 (1998).
[34]C. Noren, F. B. Yousif, and J. B. A. Mitchell, J. Chem. Soc. Faraday Trans. 2 **85**, 1697 (1989).
[35]D. R. Bates and J. B. A. Mitchell, Planet. Space Sci. **39**, 1297 (1991).
[36]H. H. Michels, "Theoretical determination of electronic transition probabilities for diatomic molecules," Technical Report AFWL-TR-72-1, May 1972.
[37]M. Fifirig, Mol. Phys. **112**, 1910 (2013).
[38]D. Spelsberg and W. Meyer, J. Chem. Phys. **115**, 6438 (2001).
[39]Y. Morioka, Y. Lu, T. Matsui, T. Tanaka, H. Yoshii, T. Hayaishi, and R. I. Hall, J. Chem. Phys. **104**, 9357 (1996).
[40]Y. Bing and F. Wei, Chin. Phys. B **19**, 033303 (2010).
[41]S. L. Guberman, J. Phys. Chem. A **111**, 11254 (2007).
[42]D. A. Little and J. Tennyson, J. Phys. B **46**, 145102 (2013).
[43]M. Hochlaf, H. Ndome, D. Hammoutène, and M. Vervloet, J. Phys. B **43**, 245101 (2010).
[44]T. H. Dunning, Jr., J. Chem. Phys. **90**, 1007 (1989).
[45]K. Kaufmann, W. Baumeister, and M. Jungen, J. Phys. B **22**, 2223 (1989).
[46]P. Cremaschi, A. Chattopadhyay, P. V. Madhavan, and J. L. Whitten, Chem. Phys. **109**, 117 (1986).
[47]B. R. Lewis, A. N. Heays, S. T. Gibson, H. Lefebvre-Brion, and R. Lefebvre, J. Chem. Phys. **129**, 164306 (2008).
[48]D. Cossart and C. Cossart-Magos, J. Chem. Phys. **121**, 7148 (2004).
[49]K. P. Huber and C. Jungen, J. Chem. Phys. **92**, 850 (1990).
[50]J. P. Sprengers, E. Reinhold, W. Ubachs, K. G. H. Baldwin, and B. R. Lewis, J. Chem. Phys. **123**, 144315 (2005).
[51]N. Orsini, D. G. Torr, H. C. Brinton, L. H. Brace, W. B. Hanson, J. F. Hoffman, and A. O. Nier, Geophys. Res. Lett. **4**, 431, doi:10.1029/GL004i010p00431 (1977).
[52]M. A. Biondi, Geophys. Res. Lett. **5**, 661, doi:10.1029/GL005i008p00661 (1978).
[53]P. G. Richards, J. Geophys. Res. **116**, A08307, doi:10.1029/2011JA016613 (2011).
[54]X. Li, Y. L. Huang, G. D. Flesch, and C. Y. Ng, J. Chem. Phys. **106**, 1373 (1997).
[55]The total of 726 Rydberg states quoted previously (Ref. 2) is incorrect.